S. Ho[1]

Z. Suo
Mem. ASME.

Mechanical Engineering Department,
University of California,
Santa Barbara, CA 93106-5070

Tunneling Cracks in Constrained Layers

A thin, brittle layer bonded between tougher substrates is susceptible to cracking under residual and applied stresses. Such a crack initiates from an equi-axed flaw, confined by the substrates, tunneling in the brittle layer. Although tunneling is a three-dimensional process, the energy release rate at the front of a steady-state tunnel can be computed using plane strain fields. Several technically important problems are analyzed, including tunnels in adhesive joints, shear fracture, and kinked tunnels in a reaction product layer. The concept is finally applied to microcracking in brittle matrix composites caused by thermal expansion mismatch.

Introduction

Layered materials subjected to residual and applied stresses are susceptible to cracking. Depending on the application, such cracks can either fail device or degrade material. For example, cracks in multilayer capacitors form easy conducting paths, leading to electrical leak. For metal matrix composites, microcracks in fiber coating can be the nucleation sites for fatigue cracks in the matrix. A commonly observed cracking process, tunneling, is examined in this paper.

Figure 1 illustrates a thin, brittle layer of thickness h, bonding two tougher substrates, subjected to both applied and residual stresses. If the net stress in the layer is tensile and sufficiently high, it drives pre-existing flaws to tunnel through the layer. The energy release rate at the *front*, G_F, varies from point to point, and depends on the tunnel length a. A long tunnel ($a/h \to \infty$) reaches a *steady-state*: the front self-adjusts to a shape such that G_F is the same at every point along the front, which no longer depends on the tunnel length, nor on the initial flaw geometry. This steady-state energy release rate is denoted as G_{ss} in Fig. 1.

Two facts, to be elaborated upon later suggest that G_{ss} is suitable for design of constrained thin layers. First, G_{ss} is relatively easy to compute (only plane-strain analyses are required). Second, the steady-state is readily reached if pre-existing flaw size is close to layer thickness. These concepts have evolved from studies of layered materials of many varieties: composite laminates (Parvizi et al., 1978; Wang, 1984; Dvorak and Laws, 1986; Fang et al., 1989), thin films (Gille, 1985; Hu et al., 1988; Bueth, 1992; Ye et al., 1992), and brittle adhesive layers (Suo, 1990).

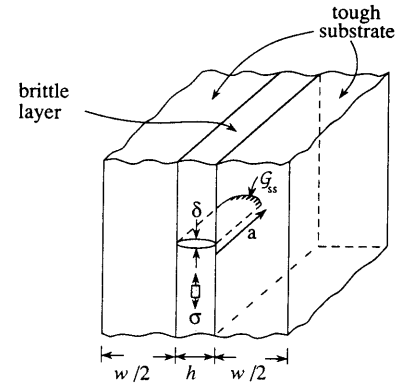

Fig. 1 A crack tunnels in a bonded layer

In this paper a new formula for G_{ss}, convenient for finite element analyses, is presented. We then discuss tunnel nucleation and the relevance of G_{ss} in design. The versatility of the concepts is demonstrated by several technically significant problems, including cracking in adhesive joints, shear fracture, and kinked cracks. The concepts are finally applied to microcracking in brittle matrix composites caused by thermal expansion mismatch.

Driving Force for Steady-State Tunneling

As sketched in Fig. 1, tunneling is a three-dimensional process. However, when the steady-state is reached, i.e., as $a/h \to \infty$, G_{ss} can be calculated using plane-strain elasticity solutions. Two alternative formulas are derived below. The tunnel is assumed to be perfectly constrained at the edges so that neither interface nor substrates crack. The significance of interface debonding and substrate cracking is reported elsewhere (Ye et al., 1992).

For such a semi-infinite tunnel the process that the front advances a unit distance is equivalent to (i) remove a unit thickness of material far ahead of the tunnel and, (ii) append a unit thickness of material in the wake. Let U be the difference in the strain energy stored in the two slices. By definition, it follows that

---

[1] Present address: Department of Theoretical and Applied Mechanics, University of Illinois, Urbana, IL 61801.

Contributed by the Applied Mechanics Division of THE AMERICAN SOCIETY OF MECHANICAL ENGINEERS for publication in the ASME JOURNAL OF APPLIED MECHANICS.

Discussion on this paper should be addressed to the Technical Editor, Professor Lewis T. Wheeler, Department of Mechanical Engineering, University of Houston, Houston, TX 77204-4792, and will be accepted until four months after final publication of the paper itself in the ASME JOURNAL OF APPLIED MECHANICS.

Manuscript received by the ASME Applied Mechanics Division, May 30, 1991; final revision, Aug. 17, 1992. Associate Technical Editor: F. Y. M. Wan.

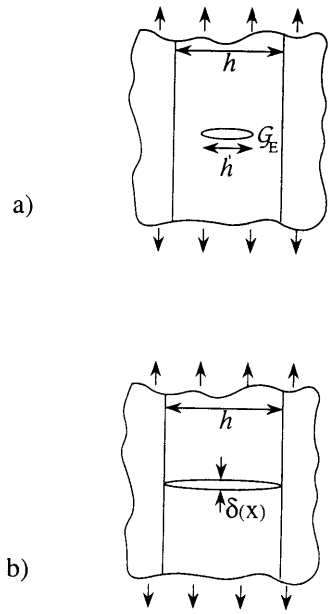

Fig. 2 *(a)* **A plane-strain crack of size $h' < h$ used for formula (2); *(b)* a plane-strain crack of size h used for formula (3)**

$$G_{ss} = U/h. \tag{1}$$

Observe that U equals the strain energy increase, at constant applied stress, due to introduction of a plane-strain crack in the unit slice. Let G_E be the energy release rate at the *edge* of a plane-strain crack of width $h' < h$ (Fig. 2(*a*)). It has been shown that (Gille, 1985; Dvorak and Laws, 1986)

$$G_{ss} = \frac{1}{h}\int_0^h G_E(h')dh'. \tag{2}$$

This formula requires G_E for plane-strain cracks of *various* width, $0 < h' < h$. As pointed out by these authors, such information is available in the literature only for a few inhomogeneous systems within limited parameter ranges, and finite element computation of G_E for various crack lengths is tedious.

Alternatively, U equals the work done by the stress through the crack opening (Fig. 2(*b*)), so that

$$G_{ss} = \frac{1}{2h}\int_0^h \sigma(x)\delta(x)dx. \tag{3}$$

Here $\sigma(x)$ is the stress distribution on the prospective crack plane prior to cracking; and $\delta(x)$ is the opening profile in the wake. Although (2) and (3) are equivalent, the latter is considerably more efficient in computation, since only two instead of many configurations need be analyzed: the stress in the uncracked body and the displacement for a plane-strain crack of *final width* h (Fig. 2(*b*)). Each of the two independent problems is under plane-strain conditions readily analyzed by commercial finite element codes.

Both (2) and (3) are valid for linear elastic systems uniform in geometry, material, and loading along the tunneling direction. In the following, (2) is used if G_E for the corresponding plane-strain cracks, with width varying from zero to the final tunnel size, is available in the literature; but (3) is used whenever finite element analysis is required.

Tunnel Nucleation

Tunnel nucleation is a complicated process. The nature of pre-existing flaws plays a predominant role—a gas bubble would behave differently from a microcrack. Several idealizations are invoked as follows. The pre-existing flaw is taken

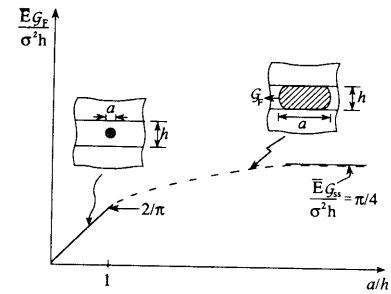

Fig. 3 The frontal energy release rate increases with the tunnel length, approaching quickly to an asymptote

to be a penny-shaped crack of initial diameter, a_0, less than layer thickness (Fig. 3). Some time-dependent subcritical cracking mechanism is assumed, so that the flaw grows slowly into a long tunnel under a constant applied stress, σ. The thin layer and the substrates are assumed to have identical elastic constants, and substrates are semi-infinite. The main objective of the following discussion is to provide a rough estimate of the tunnel length needed to attain the steady-state. None of the foregoing simplifications will change the conclusions qualitatively.

Let a be the current size of the crack (Fig. 3). When $a/h < 1$, the growing crack remains penny-shaped, since the energy release rate is the same at every point along the front. This energy release rate is given by (Tada et al., 1985)

$$G_F = \frac{2}{\pi}\sigma^2 a/\bar{E} \tag{4}$$

with $\bar{E} = E/(1-\nu^2)$, E and ν being Young's modulus and Poisson's ratio. Equation (4) is the straight line in Fig. 3, up to $a/h = 1$. After touching the interfaces, the crack is confined by the tough substrates and becomes noncircular, so that (4) is not valid when $a/h > 1$.

The crack will finally become a long tunnel and reach the steady-state. To compute G_{ss}, the classical solution is needed for G_E of a plane-strain crack of width h' (Fig. 2(*a*)):

$$G_E = \frac{\pi}{2}\sigma^2 h'/\bar{E}. \tag{5}$$

Integral (2) gives

$$G_{ss} = \frac{\pi}{4}\sigma^2 h/\bar{E}. \tag{6}$$

This result is indicated in Fig. 3 as the asymptotic value for $a/h \to \infty$.

Observe that the solutions for two limiting cases, $a/h = 1$ and $a/h \to \infty$, differ only by 23 percent. Consequently, for practical purposes, the tunnel attains the steady-state as soon as $a/h \sim 1$. The fact that the solution around $a/h \approx 1$ depends on the initial flaw geometry and the growth law of subcritical cracking discourages further elaboration in this region. The dashed line in Fig. 3 is the anticipated trend.

Now consider a brittle layer without subcritical cracking mechanism, but with a well-defined fracture energy Γ—that is, the crack will not grow if $G_F < \Gamma$. Following Dvorak and Laws (1986), we distinguish *thin* and *thick* layers by the ratio of the pre-existing flaw size to the layer thickness, a_0/h.

For a *thick* layer, where $a_0/h \ll$, the critical stress for the flaw to grow is governed by the flaw size

$$\sigma_c = (\pi\Gamma\bar{E}/2a_0)^{1/2}. \tag{7}$$

As suggested by Fig. 3, under a constant applied stress $\sigma = \sigma_c$, the flaw grows dynamically into a long tunnel. For example, the flaw size for a dense ceramic scales with grain diameter, typically $a_0 = 1 \sim 10$ μm. If the layer thickness is much larger than the grain diameter, the stress needed to nucleate a tunnel

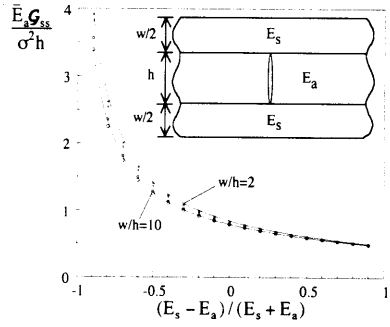

Fig. 4 Driving force for tunneling in an adhesive layer

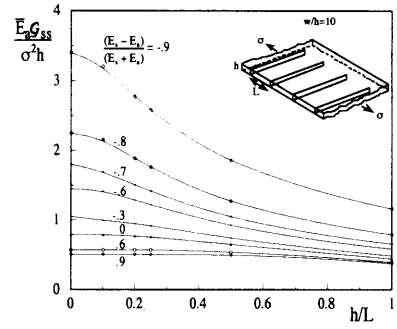

Fig. 5 Driving force for periodic tunnels

is given by (7). Consequently, the critical stress for a thick layer is identical to the strength of the material in bulk.

For a *thin* bonded layer, where the pre-existing flaws are on the other of layer thickness, i.e., $a_0/h \sim 1$, the steady-state energy release rate G_{ss} becomes relevant. From (6), one finds that the critical stress to maintain tunnel growth is

$$\sigma_c = (4\Gamma\bar{E}/\pi h)^{1/2}. \tag{8}$$

This critical stress is well defined: no knowledge of flaw geometry or microstructure is needed. It is conservative: any flaw, regardless of its initial size or shape, cannot grow into a long tunnel if the applied stress is below σ_c. Consequently, the critical stress derived from G_{ss} can serve as a well-defined, conservative design criterion for avoidance of tunnel cracks in brittle thin layers. It is clear from Fig. 3 that the criterion becomes overly conservative for very thick layers ($a_0/h \ll 1$).

Observe that the critical stress (8) is governed by layer thickness; the thinner the layer, the higher the strength, everything else being equal. This has motivated the conception of microlaminates, consisting of alternate metal and ceramic, each layer submicron thick, fabricated by a variety of thin film deposition techniques (Evans, private communication). Because cracks in a ceramic layer are confined by the adjacent metal layers, and dislocations in a metal layer is confined by the adjacent ceramic layers (Freund, 1990), the microlaminates can have very high elastic limit, unprecedented by bulk solids.

The rest of the paper will focus on applying tunneling concepts to a variety of technical problems, with nucleation stage ignored. Each individual application of the following results must be validated on the basis that the pre-existing flaw size is close to the layer thickness.

Adhesive Layer

Inserted in Fig. 4 is a cross-section of a tunnel wake. In finite element calculations, Poisson's ratios are taken to be $\nu_a = \nu_s = 1/3$, so that elastic mismatch is specified by $(E_s - E_a)/(E_s + E_a)$. The plane-strain conditions prevail in the tunnel wake. We analyze the plane-strain field using finite elements; the computed opening profile is integrated according to (3). The normalized G_{ss} is plotted in Fig. 4, varying the elastic mismatch and thickness ratio. Substrate thickness has little effect; the curve for semi-infinite substrates is nearly identical to the curve for $w/h = 10$ with the resolution of Fig. 4. Figure 4 is therefore sufficiently complete for practical purposes. The following illustrates an application.

In an experiment by Zdaniewski et al. (1987), different glasses were used to bond alumina substrates. Gas bubbles of size of layer thickness formed in the glass during bonding, acting as tunnel nuclei. The residual stresses for the four glasses used in the experiment were $\sigma_R = 63, 50, 131, 132$ MPa, respectively. Tunnels were observed to radiate from the bubbles in the last two glasses, but not the first two. Take $E_{\text{glass}} = 70$ GPa and $E_{\text{alumina}} = 350$ GPa. From Fig. 4, this elastic mismatch corresponds to $G_{ss}\bar{E}_a/\sigma^2 h = 0.6$. Given that $h = 50$ μm and $\Gamma_{\text{glass}} = 5$ Jm^{-2}, the predicted critical stress is $\sigma_c = 120$ MPa. The predicted critical stress indeed discriminates glass layers with and without tunnels.

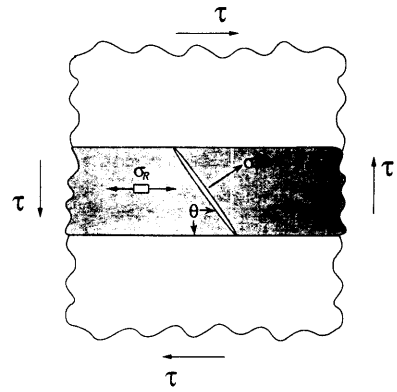

Fig. 6 Microcrack under combined residual stress and applied shear

Periodic Tunnels

Periodic tunnels can form under uniaxial tension (e.g., Parvizi et al., 1978; Laws and Dvorak, 1988). Figure 5 illustrates tunnels with spacing L. The opening profile, $\delta(x)$, is for one of the cracks which is computed using finite elements. The computed energy release rate G_{ss} is plotted in Fig. 5 for $w/h = 10$. Observe that, except for very compliant substrates, G_{ss} does not vary substantially with spacing L/h. Consequently, once the stress is sufficient to drive one tunnel, many tunnels will follow with a slightly higher stress, so long as the nucleation sites are readily available.

In Fig. 5, all the cracks are assumed to tunnel simultaneously. With a proper rearrangement of the results in Fig. 5, the driving force for new tunnels forming between existing tunnels can also be obtained (Hutchinson and Suo, 1992).

Shear Fracture

Upon closer examination of shear fracture in a laminate, one sees microcracks normal to the principal tensile stress nucleate and connect, causing macroscopic fracture (Chai, 1988). As an example consider a brittle thin layer bonded between tough substrates, subjected to shear stress τ and residual stress σ_R (Fig. 6). The larger principal stress, σ_1, and the angle between the interface and the plane of the principal stress, θ, are given by

$$\tan\theta = \sigma_1/\tau = \sigma_R/2\tau + \sqrt{(\sigma_R/2\tau)^2 + 1}. \tag{9}$$

Regardless of the sign of σ_R, σ_1 is always tensile; $\theta < 45$ deg if $\sigma_R < 0$, and $\theta > 45$ deg if $\sigma_R > 0$.

A tunnel is assumed to form perpendicular to σ_1. For simplicity, the elastic moduli of the substrates and the bonded

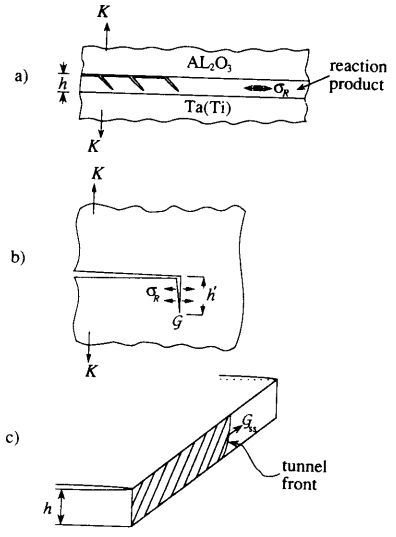

Fig. 7 Kinked tunnels

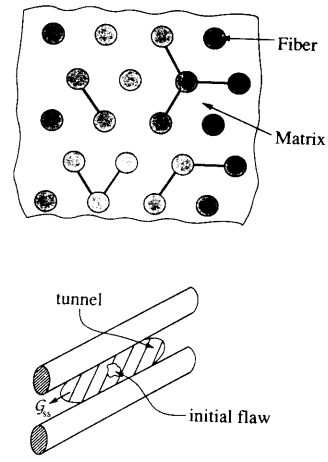

Fig. 8 Matrix cracking due to thermal mismatch

layer are taken to be identical and substrates are semi-infinite. The cross-section of the tunnel wake is a Griffith crack, so that (6) is applicable. Identifying the net stress σ_1 and tunnel width $h/\sin\theta$, one obtains

$$G_{ss}\bar{E}/h\tau^2 = \frac{\pi}{4}\sin\theta/\cos^2\theta. \tag{10}$$

For layers with different elastic constants, the tunnel angle should still be determined by (9), but finite element analysis is needed to calculate G_{ss}. Judged from Fig. 4, however, the results should be insensitive to elastic mismatch if substrates are stiffer than the layer.

Kinked Tunnels

When a Al_2O_3 plate is diffusion bonded to a Ta(Ti) alloy, a reaction product layer (RPL) of thickness 2 μm forms (He et al., 1991). The system debonds along the Al_2O_3-RPL interface upon loading, leaving behind a trail of microcracks in the RPL (Fig. 7(*a*)).

The tunnel is driven by the stress intensity at the parent crack front, K, and by the residual stress in the layer, σ_R. For simplicity the remote load is assumed to be mode I, and the microcracks are taken to be perpendicular to the interface. The system is taken to be elastically homogeneous and the two substrates are semi-infinite. None of these assumptions will affect the conclusions qualitatively.

For a kink of depth h' under the plane-strain conditions (Fig. 7(*b*)), the stress intensity factor is (He et al., 1991)

$$K_I = 0.374K + 1.766\sigma_R\sqrt{h'},\quad K_{II} = -0.347K + 0.201\sigma_R\sqrt{h'}. \tag{11}$$

The energy release rate at the kink tip can be computed from Irwin's relation

$$G_E = (K_I^2 + K_{II}^2)/\bar{E}. \tag{12}$$

The energy release rate at the tunnel front G_{ss} (Fig. 7(*c*)) can be integrated according to (2), giving

$$\bar{E}G_{ss}/K^2 = 0.260 + 0.788\eta + 1.58\eta^2,\quad \eta = \sigma_R\sqrt{h}/K. \tag{13}$$

The parameter η reflects the effect of the residual stress. When a tunnel forms, the residual tension is locally relieved. As the interface crack grows further, the residual tension recovers, driving a new tunnel.

Kinked tunnels were also observed by Chai (1987) in an epoxy bonded between aluminum substrates. He observed that the main crack ran alternating on the two interfaces, leaving behind a wavy fracture surface. This did not happen in the system of He et al. (1991), presumably because the Ta(Ti)-RPL interface is much tougher.

Thermal Cracking in Brittle Matrix Composites

All previous examples are related to layered materials. But tunneling is more prevalent. To illustrate, consider matrix cracking caused by thermal mismatch. An intermetallic reinforced by ceramic fibers, such as $MoSi_2$-SiC, usually has higher thermal expansion coefficient in the matrix than in the fibers. Upon cooling from the processing temperature, the matrix is subjected to tensile hoop stress and susceptible to cracking (Lu et al., 1991). One experimental finding is that cracking is more likely to occur in the matrix reinforced by fibers of larger radius, so that a critical fiber radius exists, below which matrix cracking is suppressed.

Focus on the radial crack in Fig.8. The thermal mismatch strain is

$$\epsilon_0 = \int_{T_r}^{T_p}(\alpha_m - \alpha_f)dT, \tag{14}$$

where α_m and α_f are thermal expansion coefficients of the matrix and fiber, and T_p and T_r are the processing temperature and room temperature. The residual stress estimated from the mismatch strain for $MoSi_2$-SiC is high ($\sim$2 GPa), well in excess of the bulk strength of $MoSi_2$. Also note that the residual stress is *independent* of fiber radius for a fixed fiber volume. These two facts eliminate the possibility of explaining the experimental finding on the basis of bulk strength.

We assume porosity exists, of size limited only by the fiber spacing, which tunnels through the matrix under sufficiently high thermal stress (Fig. 8). On dimensional grounds, the steady-state energy release rate takes the form

$$G_{ss} = \Omega\epsilon_0^2 E_m R, \tag{15}$$

where R is fiber radius and E_m is the Young's modulus of the matrix. The dimensionless prefactor, Ω, depends on fiber volume fraction, fiber arrangement, elastic mismatch, and interface properties, which has been computed using finite elements on the basis of the tunneling crack concepts developed in the previous sections (Ho and Suo, 1992).

The tunnel will not form if $G_{ss} < \Gamma_m$, Γ_m being the fracture energy of the matrix. Thus (15) gives

$$\Gamma_m/\epsilon_0^2 E_m R > \Omega. \tag{16}$$

The dimensionless group on the left-hand side consists of measurable parameters and predicts, among other things, that the larger the fiber radius, the more likely will the matrix crack, which is in agreement with the experimental findings.

Concluding Remarks

Cracks tunnel in confined geometries. The steady-state tunneling defines a conservative design limit. The energy release rate at the tunnel front is computed for a number of cases. To demonstrate the versatility of the concepts without going into technical details we have treated each problem in its simplest form. Many more computations are needed to take key variables into account, so that rigorous design criteria will emerge. Nevertheless, results presented here can be used as a base line for such purposes. Although this paper has focused on cracking in brittle layers, tunnels can form in ductile metal or polymer layers under cyclic loading. The fatigue life is dictated by the steady-state energy release rate, provided large flaws are available and tunnels do not take many cycles to nucleate.

Acknowledgment

Support is provided by ONR/URI contract N-0014-92-J-1808, and by NSF Young Investigator Award MSS-9258115. Finite element analyses are carried out using ABAQUS.

References

Beuth, J. L., 1992, "Cracking of Thin Bonded Films in Residual Tension," *Int. J. Solids and Structures*, Vol. 29, pp. 1657-1675.

Chai, H., 1987, "A Note on Crack Trajectory in an Elastic Strip Bounded by Rigid Substrates," *Int. J. Fracture*, Vol. 32, pp. 211-213.

Chai, H., 1988, "Shear Fracture," *Int. J. Fracture*, Vol. 37, pp. 137-159.

Dvorak, G. J., and Laws, N., 1986, "Analysis of First Ply Failure in Composite Laminates," *Engng. Fracture Mech.*, Vol. 25, pp. 763-770.

Dvorak, G. J., and Laws, N., 1988, "Progressive Transverse Cracking in Composite Laminates," *J. Composite Materials*, Vol. 22, pp. 900-916.

Fang, G. P., Schapery, R. A., and Weitsman, Y., 1989, "Thermally-Induced Fracture in Composites," *Engng. Fracture Mech.*, Vol. 33, pp. 619-623.

Freund, L. B., 1990, "The Driving Force for Gliding of a Threading Dislocation in a Strained Epitaxial Layer on a Substrate," *J. Mech. Phys. Solids*, Vol. 38, pp. 657-679.

Gille, G., 1985, "Strength of Thin Films and Coatings," *Current Topics in Materials Science*, Vol. 12, E. Kaldis, ed., North Holland, Amsterdam.

He, M.-Y., Bartlett, A., Evans, A. G., and Hutchinson, J. W., 1991, "Kinking of a Crack Out of an Interface: Role of In-Plane Stress," *J. Am. Ceram. Soc.*, Vol. 74, pp. 767-771.

Ho, S., and Suo, Z., 1992, "Microcracks Tunneling in Brittle Matrix Composites Driven by Thermal Expansion Mismatch," *Acta. Mer. Mater.*, Vol. 40, pp. 1685-1690.

Hu, M. S., Thouless, M. D., and Evans A. G., 1988, "The Decohesion of Thin Films from Brittle Substrates," *Acta Met.*, Vol. 36, pp. 1301-1307.

Hutchinson, J. W., and Suo, Z., 1992, "Mixed-Mode Cracking in Layered Materials," *Advances in Applied Mechanics*, Vol. 29, pp. 63-191.

Lu, T. C., Yang, J., Suo, Z., Evans, A. G., Hecht, R., and Mehrabian, R., 1991, "Matrix Cracking in Intermetallic Composites Caused by Thermal Expansion Mismatch," *Acta. Metall. Mater.*, Vol. 39, pp. 1883-1890.

Parvizi, A., Garrett, K. W., and Bailet, J. E., 1978, "Constrained Cracking in Glass Fiber-Reinforced Epoxy Cross-Ply Laminates," *J. Matter Sci.*, Vol. 13, pp. 195-201.

Suo, Z., 1990, "Failure of Brittle Adhesive Joints," ASME *Applied Mechanics Reviews*, Vol. 43, pp. S276-S279.

Tada, H., Paris, P. C., and Irwin, G. R., 1985, *The Stress Analysis of Cracks Handbook*, Del Research, St. Louis, MO.

Wang, A. S. D., 1984, "Fracture Mechanics of Sublaminate Cracks in Composite Materials," *Composite Tech. Rev.*, Vol. 6, pp. 45-62.

Ye, T., Suo, Z., and Evans, A. G., 1992, "Thin Film Cracking and the Roles of Interface and Substrate," *Int. J. Solids Structures*, Vol. 29, pp. 2639-2648.

Zdaniewski, W. A., Conway, J. C., and Kirchner, H. P., 1987, "Effects of Joint Thickness and Residual Stresses on the Properties of Ceramic Adhesive Joints," *J. Am. Ceram. Soc.*, Vol. 70, pp. 104-109.